Inorganic Chemistry
Article

Inorg. Chem. **2011**, *50*, 193–200 **193**
DOI: 10.1021/ic101651p

Investigation of the Formation of $CuInS_2$ Nanoparticles by the Oleylamine Route: Comparison of Microwave-Assisted and Conventional Syntheses

Andreas Pein,[†,‡] Mostafa Baghbanzadeh,[§,#] Thomas Rath,[†,‡] Wernfried Haas,[‡,∥] Eugen Maier,[†] Heinz Amenitsch,[⊥] Ferdinand Hofer,[∥] C. Oliver Kappe,[*,§,#] and Gregor Trimmel[*,†,‡]

[†]*Institute for Chemistry and Technology of Materials, Graz University of Technology, Stremayrgasse 9, 8010 Graz, Austria,* [‡]*Christian Doppler Laboratory for Nanocomposite Solar Cells, Graz University of Technology and NanoTecCenter Weiz Forschungsgesellschaft mbH, Austria,* [§]*Institute of Chemistry, University of Graz, Heinrichstrasse 28, 8010 Graz, Austria,* [#]*Christian Doppler Laboratory for Microwave Chemistry, University of Graz, Heinrichstrasse 28, 8010 Graz, Austria,* [∥]*Institute for Electron Microscopy and Fine Structure Research, Graz University of Technology, Steyrergasse 17, 8010 Graz, Austria, and* [⊥]*Institute of Biophysics and Nanosystems Research, Austrian Academy of Science, Schmiedlstrasse 6, 8042 Graz, Austria*

Received August 13, 2010

The formation of copper indium disulfide nanoparticles via the oleylamine route using copper iodide, indium chloride, and elemental sulfur has been investigated by applying conventional thermal heating as well as microwave irradiation. Oleylamine thereby acts as a capping ligand as well as a solvent. In an initial set of experiments, the onset of the reaction was determined to be around 115 °C by an in situ X-ray study using Synchrotron radiation. Using comparatively low synthesis temperatures of 120 °C, it is already possible to obtain nanoparticles of 2−4 nm with both heating methods but with irregular shape and size distribution. By applying higher temperatures of 220 °C, more crystalline and larger nanoparticles were obtained with slight differences in crystallite size and size distribution depending on the synthesis route. The size of the nanoparticles is in the range of 3−10 nm depending on the heating time. Using microwave irradiation, it is possible to obtain nanoparticles in only 90 s of total synthesis time. Control experiments to probe a nonthermal microwave effect were carried out ensuring an identical experimental setup, including the heating profile, the stirring rate, and the volume and concentration of the solutions. These experiments clearly demonstrate that for the preparation of $CuInS_2$ nanoparticles described herein no differences between conventional and microwave heating could be observed when performed at the same temperature. The nanoparticles obtained by microwave and thermal methods have the same crystal phase, primary crystallite size, shape, and size distribution. In addition, they show no significant differences concerning their optical properties.

Introduction

Copper indium disulfide, $CuInS_2$, like $CuInSe_2$, and $CuIn_xGa_ySe_2$ (CIGS), a member of the I−III−VI semiconductor family, is an interesting alternative for silicon-based photovoltaic/solar cell materials. $CuInS_2$ exhibits a suitable direct bandgap of 1.5 eV and a high absorption coefficient, and its applicability in solar cells has already been demonstrated.[1,2] Today, there is a growing interest to find low cost routes for the production of solar cell materials. Solvent-based routes leading to stable $CuInS_2$ nanoparticle dispersions are very attractive as they avoid energy intensive vacuum techniques for the production of the active material. The dispersion can be used like an "ink" and thus be applied in a broad variety of printing and coating production processes which are in addition easily scalable toward high production speed and large areas. Different synthetic methods have been investigated for the preparation of $CuInS_2$ nanoparticles. Besides solid state reactions,[3] various solution-based routes, for example, hot injection methods,[4] solvothermal routes,[5] and single-source precursor methods[6] have been applied. In particular, colloidal synthesis routes using suitable capping agents,[7] have been heavily investigated in recent years. Recently, the popular

*To whom correspondence should be addressed. (G.T.) E-mail: gregor.trimmel@tugraz.at. Tel.: ++43316-87332281. Fax ++43316-8731032331; (C.O.K.) E-mail: oliver.kappe@uni-graz.at.

(1) Nanu, M.; Schoonman, J.; Goossens, A. *Nano Lett*. **2005**, *5*, 1716.
(2) Scheer, R.; Walter, T.; Schock, H. W.; Fearheiley, M. L.; Lewerenz, H. J. *Appl. Phys. Lett*. **1993**, *63*, 3294.
(3) Carmalt, C. J.; Morrison, D. E.; Parkin, I. P. *J. Mater. Chem*. **1998**, *8*, 2209.
(4) Pan, D. C.; An, L. J.; Sun, Z. M.; Hou, W.; Yang, Y.; Yang, Z. Z.; Lu, Y. F. *J. Am. Chem. Soc*. **2008**, *130*, 5620.
(5) (a) Jiang, Y.; Wu, Y.; Mo, X.; Yu, W. C.; Xie, Y.; Qian, Y. T. *Inorg. Chem*. **2000**, *39*, 2964. (b) Yu, C.; Yu, J. C.; Wen, H.; Zhang, C. *Mater. Lett*. **2009**, *63*, 1984.
(6) (a) Castro, S. L.; Bailey, S. G.; Banger, K. K.; Hepp, A. F. *Chem. Mater*. **2003**, *15*, 3142. (b) Batabyal, S. K.; Tian, L.; Venkatram, N.; Ji, W.; Vittal, J. J. *J. Phys. Chem C*. **2009**, *113*, 15037.
(7) (a) Courtel, F. M.; Paynter, R. W.; Marsan, B.; Morin *Chem. Mater*. **2009**, *21*, 3752. (b) Czekelius, C.; Hilgendorff, M.; Spanhel, L.; Bedja, I.; Lerch, M.; Müller, G.; Bloeck, U.; Su, D.-S.; Giersig, M. *Adv. Mater*. **1999**, *11*, 643. (c) Zhong, H.; Zhou, Y.; Ye, M.; He, Y.; Ye, J.; He, C.; Yang, C.; Li, Y. *Chem. Mater*. **2008**, *20*, 6434.

Published on Web 12/08/2010

oleylamine route originally published for binary metal sulfide nanoparticles by Joo et al.[8] has been applied for $CuInS_2$ nanocrystal preparation.[9] Changing the reaction condition by using other amines, mixtures with coligands, or other sulfur sources strongly influences the crystal phase, growth, and morphology of the obtained $CuInS_2$ nanocrystals.[10] There are also two very recent reports using microwave heating for the preparation of $CuInS_2$ nanoparticles, one method using a single source precursor,[11] and another procedure utilizing an aqueous based synthesis protocol.[12] However, to our knowledge, there is no study on microwave-assisted routes to $CuInS_2$ using the oleylamine route.

In the past two decades, the use of microwave energy to heat chemical reactions has attracted a considerable amount of attention, due to its many successful applications in organic/peptide synthesis, polymer chemistry, material sciences, nanotechnology, and biochemical processes.[13,14] First reports using microwave-assisted methods in nanoparticle synthesis date back to the mid 1990s,[15] and from then on all known types of nanoscale materials, ranging from metals to oxides, chalcogenides, and phosphates, were successfully prepared using microwave technology.[16] The motivation for the use of microwave energy has mainly been to design faster, cleaner, and economically more viable methods of synthesis. If efficient agitation can be ensured,[17] and the temperature is monitored/controlled by fast-responding internal probes,[17,18] rapid "in core" volumetric heating without significant temperature gradients will occur. The very rapid heating and sometimes extreme temperatures observable in microwave chemistry generally lead to faster processes and transformations that require several hours when performed in a solvent at reflux temperature in an oil bath however may reach completion in a few minutes or even seconds using superheated solvents in a sealed vessel, autoclave-type, microwave reactor.[19,20] These unique features explain the growing popularity of this nonclassical heating method in many different fields of chemistry, including the generation of inorganic nanocrystals.[16,21−25] Regardless of the large published body of work in this field, there is still considerable controversy on the exact reasons why microwave irradiation is able to improve the synthesis of nanoparticles.[16] On the basis of the characteristics of the microwave dielectric heating phenomena,[14,18] in many of the published cases the reasons for the observed enhancements and altered nanoparticle properties comparing microwave and conventional heating are probably due to purely thermal/kinetic effects, resulting from the higher bulk reaction temperatures and more rapid heating rates that can be attained in a microwave irradiation experiment.[21] However, since the early days of utilizing microwave irradiation for nanoparticle generation,[15] the observed rate accelerations, and the often different shape and size of the derived nanoparticles, have led to speculations on the involvement of so-called "specific" microwave effects such as superheating,[22] selective heating,[23] or wall effect minimization.[24] Some authors have also suggested that so-called "nonthermal" microwave effects play a role in nanoparticle generation.[25] Unfortunately, while in organic or polymer chemistry the microwave-dependent effects can be specifically discussed in terms of the reaction trajectory,[26] the lack of an in-depth mechanistic picture for nanoparticle formation (nucleation and growth) makes the determination of the exact influence of microwave irradiation on the intermediates and transition states for nanoparticle formation more difficult.

In this manuscript, we investigate the synthesis of $CuInS_2$ nanoparticles using CuI, $InCl_3$, and elemental sulfur as precursors and oleylamine as a solvent and capping agent. Thereby, we first study the onset of nanoparticles formation at low temperatures by an in situ X-ray study using Synchrotron irradiation. The second issue focuses on the comparison of synthesis procedures using a conventional oil bath and microwave heating at different temperatures. Finally, carefully executed control experiments are undertaken to separate putative "specific" or "nonthermal" microwave effects from thermal effects during the $CuInS_2$ nanoparticle synthesis.

Experimental Section

All chemicals were purchased from Sigma Aldrich in the following purities: $InCl_3$ (98%), CuI (99.999%), elemental

(8) (a) Joo, J.; Na, H. B.; Yu., T.; Yu, J. H.; Kim, Y. W.; Wu, F.; Zhang, J. Z.; Hyeon, T. *J. Am. Chem. Soc.* **2003**, *125*, 11100. (b) Kwon, G.; Hyeon, T. *Acc. Chem. Res.* **2008**, *41*, 1696.

(9) Panthani, M. G.; Akhavan, V.; Goodfellow, B.; Schmidtke, J. P.; Dunn, L.; Dodabalapur, A.; Barbara, P. F.; Korgel, B. A. *J. Am. Chem. Soc.* **2008**, *130*, 16770.

(10) (a) Nose, K.; Soma, Y.; Omata, T.; Otsuka-Yao-Matsuo, S. *Chem. Mater.* **2009**, *21*, 2607. (b) Koo, B.; Patel, R. N.; Korgel, B. A. *Chem. Mater.* **2009**, *21*, 1962. (c) Xie, R.; Rutherford, M.; Peng, X. *J. Am. Chem. Soc.* **2009**, *131*, 5691. (d) Norako, M. E.; Franzman, M. A.; Brutchey, R. L. *Chem. Mater.* **2009**, *21*, 4299.

(11) Sun, C.; Gardner, J. S.; Shurdha, E.; Margulieux, K. R.; Westover, R. D.; Lau, L.; Long, G.; Bajracharya, C.; Wang, C.; Thurber, A.; Punnoose, A.; Rodriguez, R. G.; Pak, J. J. *J. Nanomater.* **2009**, Article ID 748567, 7 pages.

(12) Bensebaa, F.; Durand, C.; Aouadou, A.; Scoles, L.; Du, X.; Wang, D.; Le Page, Y. J. *Nanopart. Res.* **2010**, *12*, 1897.

(13) For a recent review with >900 references and a tabular survey of ca. 200 microwave chemistry review articles, books and book chapters, see Kappe, C. O.; Dallinger, D. *Mol. Diversity* **2009**, *13*, 71.

(14) For recent books, see (a) Loupy, A. *Microwaves in Organic Synthesis*, 2nd ed.; Wiley-VCH: Weinheim, 2006. (b) Kappe, C. O.; Stadler, A. *Microwaves in Organic and Medicinal Chemistry*; Wiley-VCH: Weinheim, 2005. (c) Bogdal, D.; Prociak, A. *Microwave-Enhanced Polymer Chemistry and Technology*; Blackwell Publishing: Oxford, 2007. (d) Lill, J. R. *Microwave Assisted Proteomics*; RSC Publishing: Cambridge, 2009.

(15) (a) Komarneni, S.; Katsuki, H. *J. Am. Ceram. Soc.* **1998**, *81*, 3041. (b) Hu, M. Z.-C.; Harris, M. T.; Byers, C. H. *J. Colloid Interface Sci.* **1998**, *198*, 87. (c) Spatz, J.; Mössmer, S.; Möller, M.; Kocher, M.; Neher, D.; Wegner, G. *Adv. Mater.* **1998**, *10*, 473.

(16) (a) Bilecka, I.; Niederberger, M. *Nanoscale* **2010**, *2*, 1358. (b) Polshettiwar, V.; Nadagouda, M. N.; Varma, R. S. *Aust. J. Chem.* **2009**, *62*, 16.

(17) Herrero, M. A.; Kremsner, J. M.; Kappe, C. O. *J. Org. Chem.* **2008**, *73*, 36.

(18) Obermayer, D.; Kappe, C. O. *Org. Biomol. Chem.* **2010**, *8*, 114.

(19) For a more detailed description of these processes, see (a) Gabriel, C.; Gabriel, S.; Grant, E. H.; Halstead, B. S.; Mingos, D. M. P. *Chem. Soc. Rev.* **1998**, *27*, 213. (b) Mingos, D. M. P.; Baghurst, D. R. *Chem. Soc. Rev.* **1991**, *20*, 1.

(20) Damm, M.; Glasnov, T. N.; Kappe, C. O. *Org. Process Res. Develop.* **2010**, *14*, 215.

(21) (a) Komarneni, S. *Curr. Sci.* **2003**, *85*, 1730. (b) He, Y.; Lu, H.-T.; Sai, L.-M.; Lai, W.-Y.; Fan, Q.-L.; Wang, L.-H.; Huang, W. *J. Phys. Chem. B* **2006**, *110*, 13352. (c) Pana, R.; Wu, Y.; Wang, Q.; Hong, Y. *Chem. Eng. J.* **2009**, *153*, 206. (d) Yu, W.; Tu, W.; Liu, H. *Langmuir* **1999**, *15*, 6. (e) Bilecka, I.; Elser, P.; Niederberger, M. *ACS Nano* **2009**, *3*, 467.

(22) Pol, V. G.; Langzam, Y.; Zaban, A. *Langmuir* **2007**, *23*, 11211.

(23) (a) Washington, A. L., II; Strouse, G. F. *Chem. Mater.* **2009**, *21*, 2770. (b) Washington, A. L., II; Strouse, G. F. *Chem. Mater.* **2009**, *21*, 3586. (c) Hu, X.; Gong, J.; Zhang, L.; Yu, J. C. *Adv. Mater.* **2008**, *20*, 4845.

(24) Hu, X.; Yu, J. C.; Gong, J. *J. Phys. Chem. C* **2007**, *111*, 11180.

(25) Tsuji, M.; Hashimoto, M.; Nishizawa, Y.; Kubokawa, M.; Tsuji, T. *Chem.—Eur. J.* **2005**, *11*, 440.

(26) For leading reviews, see (a) Perreux, L.; Loupy, A. *Tetrahedron* **2001**, *57*, 9199. (b) Perreux, L.; Loupy, A. In *Microwaves in Organic Synthesis*, 2nd ed.; Loupy, A., Ed.; Wiley-VCH: Weinheim, 2006; Chapter 4, pp 134−218. (c) De La Hoz, A.; Diaz-Ortiz, A.; Moreno, A. *Chem. Soc. Rev.* **2005**, *34*, 164. (d) De La Hoz, A.; Diaz-Ortiz, A.; Moreno, A. In *Microwaves in Organic Synthesis*, 2nd ed.; Loupy, A., Ed.; Wiley-VCH: Weinheim, 2006; Chapter 5, pp 219−277.

sulfur (reagent grade), oleylamine (technical grade). All chemicals were used without further purification.

Caution! *In the below described reaction, toxic and low volatile thiols can be evolved. All reactions must be undertaken under a fume hood and protective clothing must be used.*

Microwave Instrumentation. Preliminary microwave synthesis experiments were carried out using a Biotage Initiator 8 EXP (2.5) single-mode cavity instrument producing controlled microwave irradiation at 2450 MHz (Biotage AB, Uppsala). Experiments were performed in sealed Pyrex microwave vials (0−400 W maximum power) using temperature control mode. Reaction times refer to hold times at the reaction temperature indicated, not to total irradiation times. The temperature was measured with an IR sensor on the outside of the reaction vessel. Advanced microwave experiments with internal reaction temperature monitoring were performed using a Monowave 300 single-mode microwave reactor from Anton Paar GmbH (Graz, Austria). The instrument uses a maximum of 850 W magnetron output power and can be operated at 300 °C reaction temperature and 30 bar pressure. The reaction temperature is monitored either by an external infrared sensor (IR) housed in the sidewalls of the microwave cavity measuring the surface temperature of the reaction vessel, and/or by an internal fiber-optic (FO) temperature probe (ruby thermometer) protected by a borosilicate immersion well inserted directly into the reaction mixture.[27] Microwave experiments were carried out either in 10 mL Pyrex vessels or in 10 mL silicon carbide (SiC) reaction vials with magnetic stirring. The use of SiC vials shields the contents of the vessel from the electromagnetic field and therefore simulates an oil bath experiment.[27]

Synthesis of $CuInS_2$ Nanoparticles. Conventional Synthesis. CuI (1.527 g, 8.00 mmol) and $InCl_3$ (1.772 g, 8.00 mmol, 1.0 equiv) were dissolved in oleylamine (80 mL) by heating the mixture to 170 °C for 30 min. After the solution was cooled down, a solution of sulfur (1.539 g, 48.00 mmol, 6 equiv) in oleylamine (20 mL), prepared by heating to 130 °C, was added, and the resulting mixture was heated to the desired target temperature for the appropriate time period (see main text) using an oil bath. The resulting solution was cooled to ambient conditions and the particles were precipitated by addition of methanol and separated by centrifugation. The particles were washed by suspending them in methanol, separated by centrifugation, and dried under reduced pressure at ambient temperature.

Microwave Synthesis. The precursor solutions were prepared following the same procedure as described above. Subsequently, a 20 mL Pyrex vessel equipped with a stir bar was charged with 8 mL of metal salts solution and 2 mL of sulfur solution. The vessel was sealed with a septum and the reaction mixture was exposed to microwave irradiation and held at a desired temperature for the appropriate time period (see main text). The work up procedure was performed as described above.

Comparison Studies. Comparison experiments between microwave and conventional heating were carried out mixing 2.4 mL of metal salt solution with 0.6 mL of sulfur solution in either a Pyrex or SiC 10 mL reaction vessels equipped with a stir bar. The vessels were sealed with a septum and the reaction mixtures were either exposed to microwave irradiation (MW-Pyrex and MW-SiC) or immersed in a preheated oil bath at 220 °C for 15 min (Pyrex, Oil bath). After being cooled to room temperature, the same work up and purification procedure as mentioned above for conventional synthesis afforded the nanoparticles.

Characterization techniques. Powder-X-ray diffraction (XRD measurements were performed on a Siemens D-5005 powder-diffractometer (theta−theta geometry, Cu−K_α-radiation). The sample was placed on a silicon substrate and applied to a scan rate of 0.036° s^{-1} to record the patterns in the 2θ range between 10 and 80°. The diameters of the crystallites were estimated according to the broadening of the diffraction peaks using the Scherrer relationship (eq 1):

$$D_{XRD} \approx \frac{K\lambda}{\Delta(2\theta)\cos\theta} \quad (1)$$

where $\Delta(2\theta)$ is the full width at half-maximum (fwhm) of the peak in radians, θ is half of the scattering angle 2θ, λ is the wavelength of the X-rays, and K is the shape factor ($K = 0.9$ for spherical particles). In this context, it is very important to note that the Scherrer relationship is only a good approximation for spherical crystals. The size is inversely proportional to the fwhm. For the calculation, the (112)-reflection at $2\theta = 28.4°$ was used. The experimental line width was determined to be 0.12° at this 2θ position by measuring a Si-reference standard (NIST 640c).

Transmission electron microscopy (TEM) images were acquired on a Tecnai F 20 microscope (FEI Company) with a Schottky emitter, an UltraScanCCD camera, and a Gatan GIF Quantum energy filter system. Selected area electron diffraction measurements were evaluated by determination of the diffraction center and measurement of the ring radii using the method and software plug-in described by Mitchell.[28] TEM samples for imaging were prepared from a dispersion of 0.04 mg/mL particles in chloroform by putting a drop of the dispersion on a Nickel-TEM-grid with a carbon film and evaporation of the solvent. UV/vis spectra of nanoparticle solutions in chloroform (0.05 mg/mL) were measured with a Shimadzu UV-1800 spectrophotometer.

Thermogravimetric analysis (TGA) measurements were performed with a simultaneous thermal analyzer STA 449 C Jupiter from Netsch-Gerätebau GmbH (crucibles: aluminum) with a heating rate of 10 °C/min in a flow of He (50 mL/min).

The growth of the $CuInS_2$ nanocrystals was studied by in situ time-resolved wide-angle X-ray scattering (WAXS) measurements recorded at the Austrian SAXS beamline 5.2 L[29] of the Italian synchrotron center, ELETTRA, Trieste, operated at 2 GeV. For the detection of the WAXS signals in the 2θ range of 25−32°, a 1D gas detector was used. Fitting of the WAXS peaks was done with Lorentz function. The primary particle size was estimated with the Scherrer equation.

The experimental setup consisted of a reaction vessel, a peristaltic pump, tubes, and a flow-through cell situated in the center of the beam.[30] The reaction was conducted in the reaction vessel equipped with a reflux condenser and a thermometer. The reaction mixture was stirred and heated by a magnetic stirrer/heater. To pump the solution through the measuring cell, we used steel capillaries as tubes; an elastic neoprene tube was used only for a small distance directly at the peristaltic pump. The steel capillaries were isolated to reduce the temperature loss of the solution during pumping to the measuring cell. The measuring cell was heated to 80 °C and the flow rate was adjusted to 5 mL/min. The concentration of the nanoparticles in solution was 4.5 w/w%.

Results and Discussion

In this study, we investigate the formation of $CuInS_2$ nanoparticles by a modified synthesis protocol using oleylamine as a capping agent as well as a solvent. In contrast to the method by Panthani et al., no additional solvent like chlorobenzene was used.[9] For the synthesis, a solution of the metal compounds (CuI, $InCl_3$) was prepared by heating to 170 °C for

(27) (a) Obermayer, D.; Gutmann, B.; Kappe, C. O. *Angew. Chem., Int. Ed.* **2009**, *48*, 8321. (b) Gutmann, B.; Obermayer, D.; Reichart, B.; Prekodravac, B.; Irfan, M.; Kremsner, J. M.; Kappe, C. O. *Chem. Eur. J.* **2010**, *40*, 12182.

(28) Mitchell, D. R. G. *Ultramicroscopy* **2008**, *108*, 367–374.

(29) Amenitsch, H.; Bernstorff, S.; Kriechbaum, M.; Lombardo, D.; Mio, H.; Rappolt, M.; Laggner, P. *J. Appl. Crystallogr.* **1997**, *30*, 872.

(30) Argen, P.; Linden, M.; Rosenholm, J. B.; Schwarzenbacher, R.; Kriechbaum, M.; Amenitsch, H.; Laggner, P.; Blanchard, J.; Schüth, F. *J. Phys. Chem. B* **1999**, *103*, 5943.

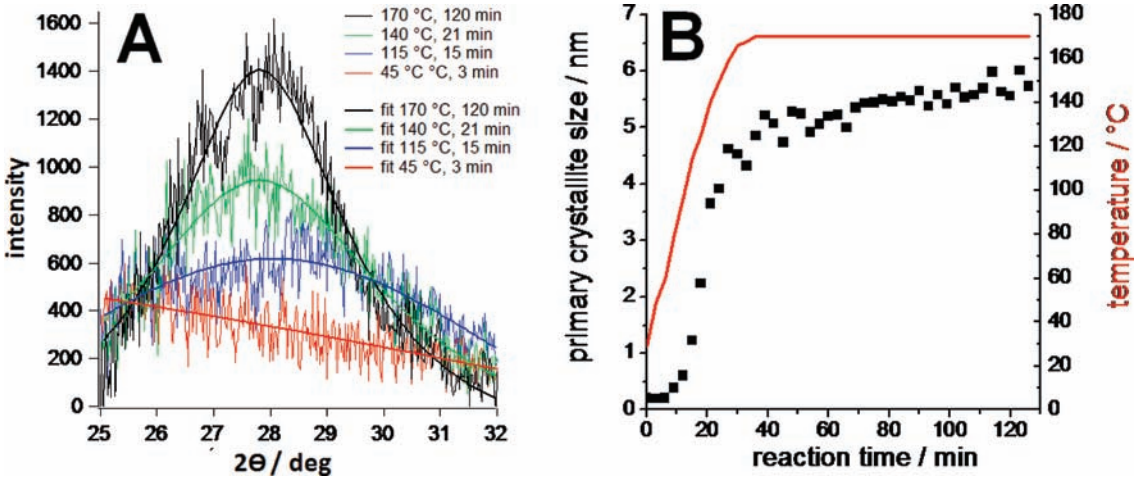

Figure 1. Wide angle X-ray scattering curves and corresponding Lorentz fits at selected temperatures (A) and primary crystallite size and temperature versus reaction time (B).

30 min in oleylamine. Separately, elemental sulfur was also dissolved in oleylamine at 130 °C. After cooling down, both solutions were combined and are subjected to different heating procedures as described in detail below.

Study of the Nanoparticle Formation by WAXS. Reaction temperatures used in the oleylamine route are usually in the range of 200 °C and above, sometimes using even autoclave conditions. To determine the lowest possible temperature for the formation of the particles, we investigated the reaction by a WAXS setup using Synchrotron radiation to obtain a high time resolution. A part of the reaction mixture was continuously pumped through a capillary directly placed in the X-ray beam. The evolution of the most intensive reflection of $CuInS_2$ at 28.1° was followed during heating the solutions from room temperature up to 170 °C using a conventional oil bath.

The results of the experiment are summarized in Figure 1. For better visibility, selected experimental data and the corresponding Lorentz fits are depicted in Figure 1A. The formation of the particles starts already at temperatures around 115−120 °C, indicated by the rise of the (112) reflection at 28.1°. Using these fits, the primary crystallite sizes were estimated by the Scherrer equation and are plotted as a function of the reaction time, as presented in Figure 1B. After 15 min − corresponding to a reaction temperature of 115 °C − the primary crystallite size starts to increase very rapidly. After 36 min, the growth rate flattens out which can be attributed to (1) a geometric factor, which means that with increasing size more monomer has to reach the particle surface to induce the same increase in particle size and (2) the decrease in educt concentration.

The WAXS analysis shows that a temperature of only 120 °C should be sufficient for the formation of $CuInS_2$ nanoparticles, which is 120 °C below the value of a literature protocol using oleylamine reported by the group of Korgel.[31]

$CuInS_2$ Nanoparticle Synthesis at 120 °C. In order to analyze the generation of $CuInS_2$ nanoparticles in a preparative way, the combined reaction mixture was heated up from room temperature to the comparatively low reaction temperature of 120 °C. Samples of the reaction solution were taken after 15 and 60 min, but also after an extended reaction time of 20 h. The time includes the heating ramp of ~15 min, and thus the 15 min sample is taken immediately after the reaction mixture has reached the target temperature of 120 °C. The nanoparticles were separated from the reaction mixture by precipitation in cold methanol and subsequent centrifugation.

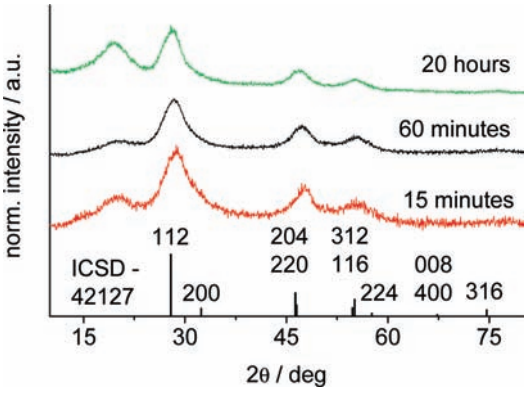

Figure 2. XRD patterns of particles prepared at 120 °C after different heating times (curves are shifted vertically for better visibility). The peaks are in good agreement with the reference file for chalcopyrite type $CuInS_2$ (ICSD − 42127 − sharp lines at the bottom).

The corresponding X-ray diffraction (XRD) patterns of these samples are compared with the reference data for $CuInS_2$ (ICSD − 42127) in Figure 2. The most prominent chalcopyrite reflections of $CuInS_2$ (Miller indexes are shown together with the reference data) are present, although the signals are noisy and broad, indicating the reduced crystallite size. Using the Scherrer equation, a primary crystallite size of 2.3 nm was calculated for nanoparticles obtained after a reaction time of 15 min. After 60 min, the particles reach a size of 2.6 nm and finally 3.7 nm after 20 h. However, the Scherrer equation can only give a rough estimation, especially for particles in the low nanometer range, but it gives an overall trend for particle size evolution. The peak around $2\theta = 18°$ can be attributed to the capping molecule, oleylamine (see Supporting Information). Interestingly, this peak is less pronounced for the first two samples (15 min, 60 min). These two samples are not soluble in nonpolar solvents, whereas the third sample and all samples prepared at 220 °C are rapidly soluble in

(31) Koo, P.; Patel, R. N.; Korgel, B. A. *Chem. Mater.* **2009**, *21*, 1962.

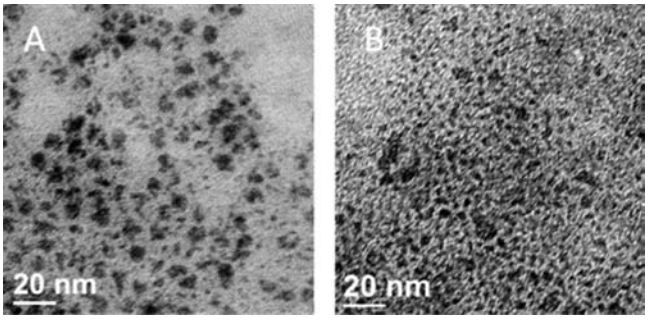

Figure 3. TEM image of $CuInS_2$ nanoparticles (A) prepared at 120 °C using conventional heating for 20 h and (B) microwave irradiation for 60 min.

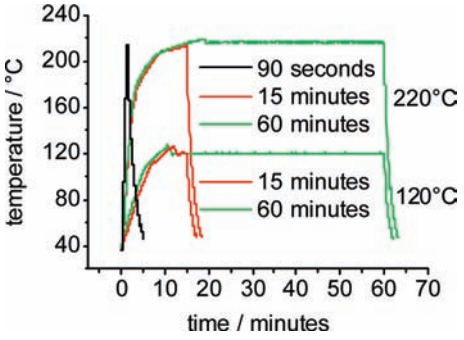

Figure 4. Heating profile of the microwave experiments at 120 and 220 °C.

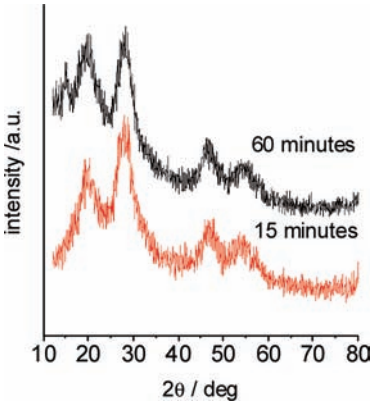

Figure 5. XRD patterns of $CuInS_2$ nanoparticles prepared using microwave heating at 120 °C times (curves are shifted vertically for better visibility).

solvents such as hexane, chloroform, and dichloromethane. At the moment, we have no explanation for this phenomenon, but the lower intensity of the XRD-peak at 2θ = 18° is an indication that less capper is retained after the work up and therefore a higher tendency of these particles to agglomerate is expected.

In Figure 3A, the TEM image of the sample prepared at 120 °C for 20 h shows nanoparticles with a diameter between 2 and 4 nm. In addition, some larger agglomerates between 5 and 10 nm are visible.

To investigate possible differences between the classical oil bath synthesis and an alternative heating mechanism by microwave irradiation, the nanoparticle synthesis was also performed in a dedicated microwave reactor at 120 °C. It should be emphasized, however, that in these preliminary experiments the heating profiles seen in the oil bath experiments were mimicked in the microwave runs by simply adjusting the instrument power, and not by an adequate algorithm that involves feedback from an internal temperature probe (see below). In addition, other important processing factors such as reaction volume, vessel geometry and stirring speed were all different (see Experimental Section for details). Importantly, the temperature measurements for both sets of experiments were different, since for the oil bath runs a traditional glass thermometer monitoring the reaction mixture temperature was used, while in the microwave experiments an external IR sensor reading the surface temperature of the Pyrex reaction vessels was employed. Reaction times refer to the overall reaction time involving ramp time (time needed to reach the target temperature) and hold time (time for which the sample is held at target temperature). The corresponding heating profiles are depicted in Figure 4. Reaction times of 15 and 60 min were applied.

Figure 5 shows the XRD patterns of the samples synthesized under microwave conditions at 120 °C. In both cases, $CuInS_2$ nanoparticles of chalcopyrite structure are obtained. According to the Scherrer equation, the particles have an average primary crystallite size of 1.8 nm after 15 min and 2.5 nm after 60 min, and thus the particle sizes are comparable with those obtained using the oil bath (2.3 nm, 15 min; 2.6 nm, 60 min). In addition, these particles contain a significant amount of organic capper (peak around 2θ = 18°) and both the samples are soluble in organic nonpolar solvents. The peak around 2θ = 15° in the 60 min sample can be attributed to a small quantity of unidentified impurities.

Figure 3B shows the TEM image of the particles prepared using microwave heating after a reaction time of 60 min. The particle size is around 3 nm but also in this case the size distribution is quite broad.

The TEM images as well as the XRD data clearly show that $CuInS_2$ nanoparticles are already formed at 120 °C using both heating methods, at much lower temperatures as usually employed for this synthesis protocol. However, the particles are rather small in size, the size distribution is broad, and the particles are irregular in shape. In order to improve the particle quality, in the next step we investigated both synthesis methods at 220 °C, a temperature which can be obtained with a conventional oil bath as well as by microwave heating.

$CuInS_2$ Nanoparticle Synthesis at 220 °C. Figure 6 shows the XRD patterns of nanoparticles prepared with oil bath heating after 15, 40, and 80 min at a temperature of 220 °C. An increase of particle size can be observed from the increase of reflections with longer reaction times. In addition, some minor intensity reflections (2θ = 57.7° and 77.1°) are now clearly visible. The primary crystallite sizes, estimated from the Scherrer equation, reach a size of 5.7 nm after 15 min, 9.4 nm after 40 min, and finally around 12.1 nm after 80 min.

The TEM image in Figure 7 shows a representative overview of the nanoparticles obtained at 220 °C using conventional heating. The particles are of angled shape and the particle size is in the range between 5 and 10 nm. Compared to the particles prepared at 120 °C (Figure 3),

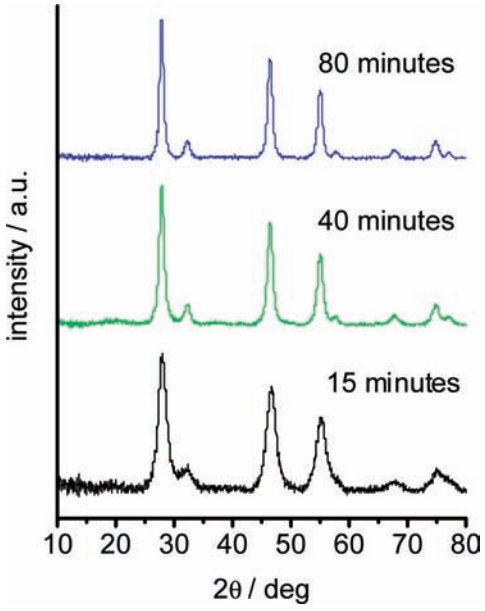

Figure 6. XRD patterns of particles prepared at 220 °C after different heating times (curves are shifted vertically for better visibility).

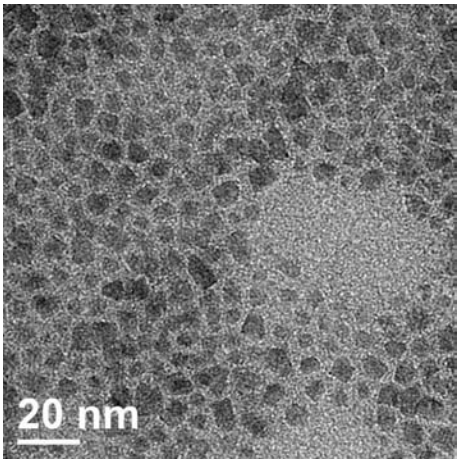

Figure 7. TEM image of $CuInS_2$ particles prepared at 220 °C using an oil bath for 15 min.

the size distribution is improved and also the shape is much more regular.

The same experiment at 220 °C target temperature was additionally undertaken using microwave irradiation. The heating profiles for these experiments are presented in Figure 4. In both cases, reaction times of 15 and 60 min were applied using a heating profile similar to conventional heating. In addition, an experiment with a very short reaction time of 90 s including 80 s ramping and 10 s heating at target temperature (high microwave power) was performed, as especially the fast heating ramp is considered to be an important asset of microwave chemistry.[12,13,15] Figure 8 compares the XRD patterns of the particles from these experiments. The crystal modification of chalcopyrite type $CuInS_2$ is also obtained in all cases. The experiment (15 min heating) with a slower heating ramp (cf. Figure 4) − approximately the same heating rate used in the oil bath experiments − yields particles with a particle size of 3.5 nm. Using prolonged microwave irradiation for an additional 45 min leads to

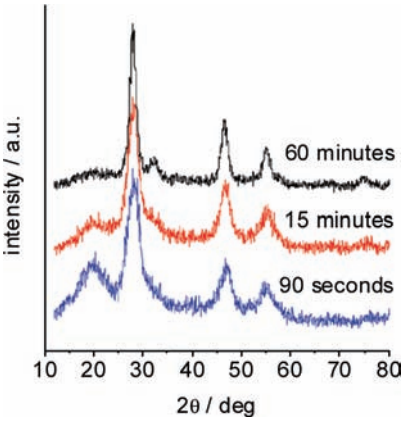

Figure 8. XRD patterns of the particles prepared using microwave heating at 220 °C (curves are shifted vertically for better visibility).

particles with a size of 6.5 nm. Interestingly, particles with a size of 3.3 nm are already obtained after 90 s heating at 220 °C. This demonstrates one of the distinct advantages of microwave chemistry, fast syntheses protocols by extremely fast heating to the desired temperatures.[13,14,16]

In Figure 9, the TEM images of these samples differ significantly from each other. In contrast to the XRD patterns, the shape and size distribution of the nanoparticles of the 90 s sample and the 15 min sample seems to be different. However, having a closer look both samples contain nanoparticles with a crystallite size of approximately 2−4 nm, but the 15 min samples show, in addition, a lot more agglomerates in the range of 6−15 nm. The particles obtained by the 60 min synthesis are very irregular and exhibit a broad size distribution with particles ranging in size from 5 to 20 nm. Comparing the TEM images in Figure 9B, the nanoparticles obtained with microwave irradiation at 15 min, and in Figure 7, the sample prepared using conventional heating, the particle size (2−3 nm compared to 5−6 nm), and the size distribution are quite different depending on the heating used. Therefore, an analysis of the above results may in fact imply the existence of a "microwave effect" in the preparation of these materials. However, as it is known that the geometry of the reaction vessel, the heating and cooling ramp, and stirring speed sometimes have a significant influence in microwave chemistry,[16,18] a series of carefully executed control experiments was designed to minimize these effects.

Comparison of Oil Bath and Microwave Heating for the $CuInS_2$ Nanoparticle Generation under Controlled Reaction Conditions. In order to accurately compare the results obtained by direct microwave heating with the outcome of a conventionally heated chemical transformation, we have recently demonstrated that the utilization of reaction vials made out of sintered silicon carbide (SiC) ceramic in microwave reactors can mimic a conventionally heated autoclave experiment, while retaining the rapid heating (flash heating) and excellent process control features inherent to microwave chemistry.[27] Since by employing a SiC vial any effects of the electromagnetic field on the reaction mixture can be eliminated, this technology makes it possible to effectively separate thermal from specific/nonthermal effects.[27] As an additional control experiment, the $CuInS_2$ nanoparticle synthesis was also performed in a conventionally heated Pyrex vial with

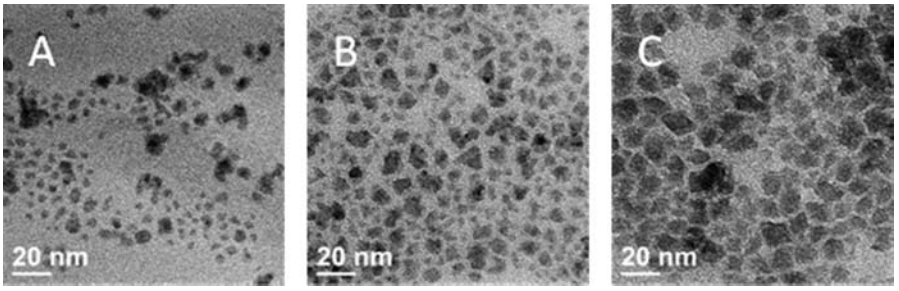

Figure 9. TEM images of the $CuInS_2$ nanoparticle samples prepared at 220 °C using microwave irradiation: (A) 90 s, (B) 15 min, and (C) 60 min experiment.

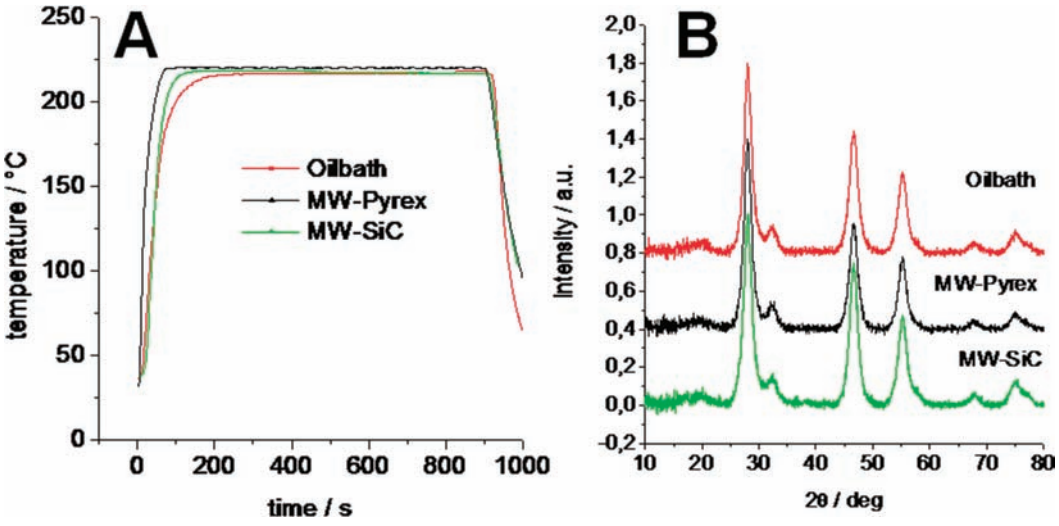

Figure 10. Heating profiles of the control experiments (A), XRD-patterns of the experiments obtained after 900 s (15 min) overall reaction time (B).

internal temperature control that allowed us to accurately mimic the heating profiles obtained in the microwave experiments.[17] Internal temperature control using fiber-optic technology was used for both microwave and conventionally heated runs since recent evidence has demonstrated that monitoring reaction temperatures by conventional infrared sensors on the outside vessel wall is not an acceptable technique if an accurate temperature profile for comparison studies needs to be obtained.[17,18,32] Since oleylamine is a solvent of comparatively low microwave absorptivity,[19] the pure solvent alone cannot be heated to high temperatures (>200 °C) under microwave conditions. In contrast, the reaction mixture can be easily heated to 220 °C within 2 min, indicating that the precursor−solvent complex will absorb most of the microwave energy ("selective heating").

Control experiments between microwave and conventional heating (SiC vials) were performed on a 3 mL scale using Pyrex and SiC vials in a microwave reactor under otherwise completely identical reaction conditions. The heating profiles were carefully adjusted by variation of microwave power to minimize differences resulting from a thermal effect as shown in Figure 10A. In addition, a control experiment using a preheated oil bath (bath temperature 220 °C) was performed, leading to a similar heating profile. In all cases, the desired final temperature was 220 °C and the overall heating period (including ramp and hold time) was 15 min. In Figure 10B, the corresponding XRD patterns are shown. The same reflections can be seen in all three samples and also the primary crystallite size of around 5.4 nm is in all cases identical. In order to exclude any experimental artifacts, these series of microwave and oil bath experiments were performed twice, leading to identical results.

From the TEM images, depicted in Figure 11 similar nanoparticle shapes and size distributions in the range between 5 and 10 nm can be seen for samples obtained from the three types of experiments. The only differences stem from different particle concentrations in the images. Also the SAED insets confirm the XRD results showing the diffraction rings of nonoriented nanocrystalline $CuInS_2$.

Thus, both TEM and XRD experiments cannot identify significant differences between the two heating modes. This fact was confirmed by optical absorption measurements, shown in Figure 12. Weak absorption of the nanoparticles already starts at a wavelength of around 850 nm. However, a significant increase in absorption can be observed around 500 nm, which is similar to several literature reports.[33,34]

(32) (a) Kremsner, J. M.; Kappe, C. O. *J. Org. Chem.* **2006**, *71*, 4651. (b) Hosseini, M.; Stiasni, N.; Barbieri, V.; Kappe, C. O. *J. Org. Chem.* **2007**, *72*, 1417. (c) Nüchter, M.; Ondruschka, B.; Bonrath, W.; Gum, A. *Green Chem.* **2004**, *6*, 128. (d) Leadbeater, N. E.; Pillsbury, S. J.; Shanahan, E.; Williams, V. A. *Tetrahedron* **2005**, *61*, 3565.

(33) Castro, S. L.; Bailey, S. G.; Raffaelle, R. P.; Banger, K. K.; Hepp, A. F. *J. Phys. Chem. B* **2004**, *108*, 12429.

(34) Chen, Y.; He, X.; Zhao, X.; Song, M.; Gu, X. *Mater. Sci. Eng., B* **2007**, *139*, 88.

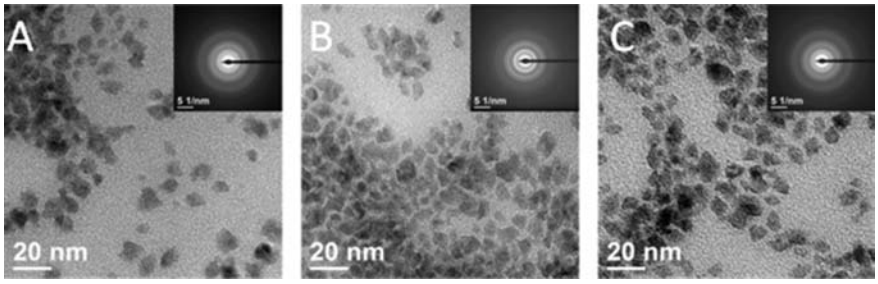

Figure 11. Comparison of TEM images and SAED pattern (inset) of the $CuInS_2$ nanoparticles synthesized at 220 °C of the (A) MW-Pyrex, (B) MW-SiC, (C) oil bath experiments. (For detailed SAED patterns see Supporting Information.)

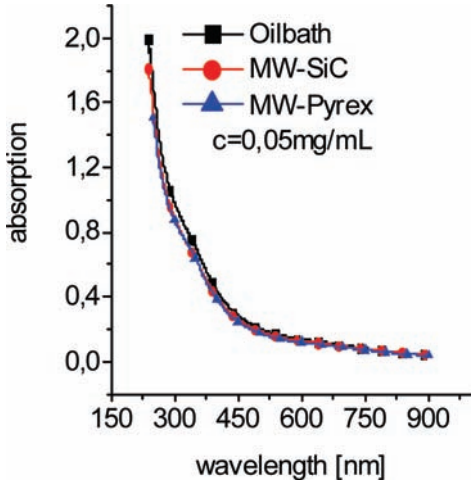

Figure 12. UV−vis spectra of the $CuInS_2$ samples synthesized at 220 °C.

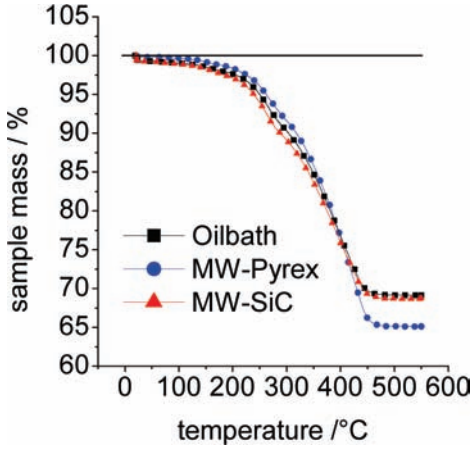

Figure 13. TGA experiments of the $CuInS_2$ samples synthesized at 220 °C.

The only small difference observed is the fact that the microwave sample has a somewhat higher amount of capping ligand, detected by thermogravimetric analysis shown in Figure 13. A mass loss due to the evaporation of the capping oleylamine of 30.7% in the case of the SiC sample, an almost identical value of 30.3% in the case of the oil bath sample and a slightly higher value of 34.7% for the Pyrex sample, was detected. Currently, we have no explanation for this reproducible effect, but further experiments are planned.

Conclusion

The formation of $CuInS_2$ nanoparticles using the oleylamine route already starts at quite low temperatures of 115−120 °C. This temperature range is far below commonly applied reaction temperatures. Both a microwave and an oil bath heating method at a temperature of 120 °C leads to small particles (approximately 2−3 nm) with irregular shape and broad size distribution. By applying higher temperatures, these quality criterions can be improved. Using microwave irradiation, it is possible to obtain nanoparticles of 3−4 nm with a reaction time of only 90 s. Although preliminary comparison experiments between microwave and conventional heating under apparently "similar" conditions performed at 120 and 220 °C have provided slightly different results in the obtained $CuInS_2$ nanoparticles, carefully executed control experiments ensuring identical heating and cooling profiles, stirring rates, and reactor geometries clearly demonstrate that for the preparation of $CuInS_2$ nanoparticles described herein no differences between conventional and microwave heating could be observed. The nanoparticles obtained by the three control experiments have the same crystal phase, primary crystallite size, shape, and size distribution and show no significant differences in absorption behavior.

Acknowledgment. The authors thank the Christian Doppler Research Association (CDG), Isovoltaic GmbH, and the Federal Ministry for Economy, Family and Youth (BMWFJ) for financial support and the Graz Centre for Electron Microscopy for support regarding the TEM measurements. WAXS experiments at the Synchrotron Elettra leading to these results have received funding from the European Community's Seventh Framework Program (FP7/2007-2013) under grant agreement 226716.

Supporting Information Available: XRD pattern of pure oleylamine and indexed SAED patterns. This material is available free of charge via the Internet at http://pubs.acs.org.